# Extended Experiments for Takeoff and Landing on Slopes via Inclined Hovering with a Tethered Aerial Robot

Technical Attachment to:
M. Tognon, A. Testa, E. Rossi and A. Franchi
"Takeoff and Landing on Slopes via Inclined Hovering with a Tethered Aerial Robot"
published in the *2016 IEEE/RSJ International Conference on Intelligent Robots and Systems*
*Daejeon, South Korea, Oct. 2016*

Marco Tognon[1], Andrea Testa[2], Enrica Rossi[1] and Antonio Franchi[1]

## I. Introduction

This document is a technical attachment to [1], a paper which provides a study and a methodology for landing and takeoff using a passive tether attached to the aerial platform. This document includes a proof of the flatness of the output $\mathbf{y}^{f_L}$ (in Section II) and extended results of the experiments not included in [1] because of page limits (in Section III).

The reader interested in the analysis and control of tethered aerial vehicles is also referred to [2], [3], where flatness, controllability and observability is studied, to [4] where the case of a moving base is thoroughly analyzed, and to [5], [6] where the case of multiple tethered vehicles is investigated.

### A. Aerial physical interaction

Tethered aerial vehicles constitute an example of aerial vehicles physically interacting with the external environment. For the reader interested in this rapidly expanding and broad topic we also suggest the reading of [7], where a force nonlinear observer for aerial vehicles is proposed, of [8], where an IDA-PBC controller is used for modulating the physical interaction of aerial robots, of [9], [10] where fully actuated platforms for full wrench exertion are presented, of [11]–[13] where the capabilities of exerting forces with a tool are studied, and finally of [14]–[16] where aerial manipulators with elastic-joint arms are modeled and their controllability properties discovered.

## II. Differential flatness with respect to $\mathbf{y}^{f_L}$

Let us consider the output $\mathbf{y}^{f_L} = [y_1^{f_L}\ y_2^{f_L}\ y_3^{f_L}\ y_4^{f_L}]^T = [\varphi\ \delta\ f_L\ \psi_R]^T \in \mathbb{R}^4$. In this section we shall demonstrate that the tethered system in [1] is differential flat with respect to $\mathbf{y}^{f_L}$. For this purpose the state and the inputs have to be written as an algebraic function of the output and its derivatives.

[1]LAAS-CNRS, Université de Toulouse, CNRS, Toulouse, France, mtognon@laas.fr, erossi@laas.fr, antonio.franchi@laas.fr
[2]Department of Engineering, Università del Salento, via per Monteroni, 73100 Lecce, Italy andrea.testa@unisalento.it
Partially funded by the European Union's Horizon 2020 research and innovation programme under grant agreement No 644271 AEROARMS.

We get directly that $\mathbf{q} = [y_1^{f_L}\ y_2^{f_L}]^T$ and $\dot{\mathbf{q}} = [\dot{y}_1^{f_L}\ \dot{y}_2^{f_L}]^T$. Then from (4) in the paper, we can write $f_R$ and $\mathbf{z}_R$ as an algebraic function of $\mathbf{y}^{f_L}$ and its derivatives as:

$$f_R = \left\|\mathbf{f}_R(\mathbf{y}^{f_L}, \dot{\mathbf{y}}^{f_L}, \ddot{\mathbf{y}}^{f_L})\right\|, \quad \mathbf{z}_R = \frac{\mathbf{f}_R(\mathbf{y}^{f_L}, \dot{\mathbf{y}}^{f_L}, \ddot{\mathbf{y}}^{f_L})}{\left\|\mathbf{f}_R(\mathbf{y}^{f_L}, \dot{\mathbf{y}}^{f_L}, \ddot{\mathbf{y}}^{f_L})\right\|}, \quad \text{(TR.1)}$$

where $\mathbf{f}_R = -m_R\ddot{\mathbf{p}}_R(\mathbf{y}^{f_L}, \dot{\mathbf{y}}^{f_L}, \ddot{\mathbf{y}}^{f_L}) - m_R g\mathbf{z}_W - y_3^{f_L}\mathbf{d}(\mathbf{y}^{f_L})$. Equation (TR.1), together with $y_4^{f_L}$, let us define the attitude of the vehicle as a function of $\mathbf{y}^{f_L}$ and its derivatives. In fact, given $y_4^{f_L}$ we can define $\mathbf{x}'_R = \mathbf{R}_{\mathbf{z}}(y_4^{f_L})\mathbf{e}_1$, where $\mathbf{R}_{\mathbf{z}}(y_4^{f_L})$ is the rotation matrix describing the rotation of $y_4^{f_L}$ along $\mathbf{z}_W$. The attitude is computed creating an orthonormal basis out of $\mathbf{x}'_R$ and $\mathbf{z}_R$, given by $\mathbf{R}_R(\mathbf{y}^{f_L}, \dot{\mathbf{y}}^{f_L}, \ddot{\mathbf{y}}^{f_L}) = [\mathbf{x}_R\ \mathbf{y}_R\ \mathbf{z}_R]$ where,

$$\mathbf{y}_R = \frac{\mathbf{z}_R \times \mathbf{x}'_R}{\|\mathbf{z}_R \times \mathbf{x}'_R\|}, \qquad \mathbf{x}_R = \frac{\mathbf{y}_R \times \mathbf{z}_R}{\|\mathbf{y}_R \times \mathbf{z}_R\|}.$$

Differentiating $\mathbf{R}_R(\mathbf{y}^{f_L}, \dot{\mathbf{y}}^{f_L}, \ddot{\mathbf{y}}^{f_L})$ and using (2) of [1], we can write $\boldsymbol{\omega}_R$ and $\boldsymbol{\tau}_R$ as a function of $\mathbf{y}^{f_L}$ and its derivatives. Finally, we were able to write state and inputs as a function of $\mathbf{y}^{f_L}$ and its derivatives, thus proving the differential flatness of the system with respect to $\mathbf{y}^{f_L}$.

## III. Full Experiment with surface tilted by 50[°]

In this section we show the main results of an experimental campaign aimed at validating the efficacy of our method for the problem of landing (and takeoff) an aerial vehicle on a sloped surface.

The goal of the experiment is to automatically land the robot on a surface, tilted by 50[°]. As already explained in [1] The maneuver starts with the vehicle in a free-flight configuration and consists of seven phases:

(a) approach to the anchor point making the hook in contact with the anchoring horizontal cable,
(b) hook the horizontal cable,
(c) stretch the link making it taut,
(d) landing with the tethered approach (see Fig. 2),
(e) turn-off the propellers after the landing,
(f) takeoff with the tethered approach,
(g) de-hooking from the anchoring cable.

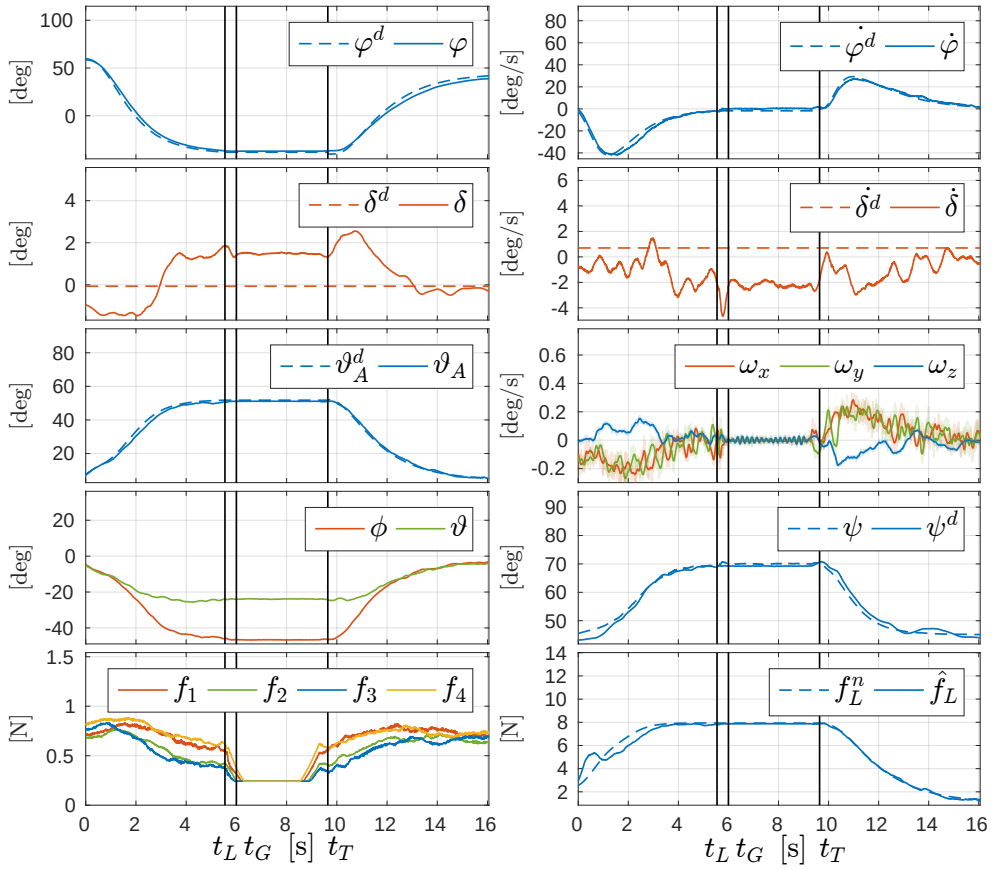



Fig. 1: Tracking of the desired landing and takeoff maneuver for a surface tilted by 50[°]. In the plot of $\boldsymbol{\omega}_R$, the solid and opaque lines correspond to the filtered and unfiltered data, respectively. $f_L^n$ is the nominal stress given by the particular trajectory, whereas $\hat{f}_L$ is the estimated stress from the knowledge of the model, state and inputs.

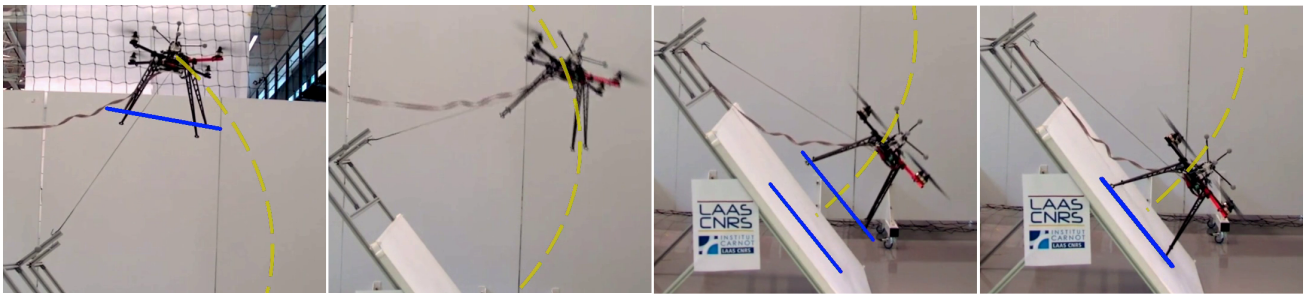



Fig. 2: Sequence of images of a real experiment during the landing maneuver (phase (d)) on a surface titled by 50[°].

Given the parameters of the system, in order to achieve the landing conditions, from Sec. III of the paper it results that:

$$\varphi^\star = -38.2[^\circ], \quad \delta^\star = 0[^\circ], \quad \vartheta_A^\star = 50[^\circ].$$

During the maneuver, $\psi_R^\star$ is set such that the frame of the vehicle is turned by 45[°] with respect to the link.

In Fig. 2 and 1 the results of the experiment are shown. At time $t_L$ the surface is reached with a stable and safe maneuver thanks to the existence of inclined equilibria (see [1]) and the motors are turned off at time $t_G$. Then, at time $t_T$ the vehicle performs the takeoff in the same safe and stable way[1].

[1]A video of the experiment is attached to [1] and also available at `https://www.youtube.com/watch?v=01UYN289YXk`

In conclusion, using the proposed method it is possible to both takeoff and land from any surfaces with different inclinations. Furthermore, it is important to notice that it is possible to attach and detach the hook from the anchor completely autonomously passing from a free-flight to tethered condition and vice versa. This lets the method be easily applied for real tasks.

## IV. Additional Experimental Tests

### A. Landing with the free-flight approach

In this paragraph we describe the results obtained trying to land on a surface tilted by 30[°] using the free-flight approach. In particular we want to show that using a classical position controller is not possible to land on such sloped



(a) Desired landing position on the surface.



(b) Desired landing position below the surface. The picture shows the vehicle the instant before crashing on the surface.

Fig. 3: Landing with the free-flight approach.

surfaces. Indeed, as demonstrated in the paper, this is possible only using a maneuver based approach, for which the landing is achieved only carefully planning the trajectory and precisely tracking it.

The dynamic of the experiment is quite simple. The vehicle starts in free-flight condition and tries to land on a desired point of the surface following a simple descending trajectory along $\mathbf{z}_W$. Finally, the robot switches off the motors when the surface is reached.

Giving as desired position a point on the surface, the vehicle touches it with only two landers and remains in an almost hovering condition (see Fig. 3a). Then, when the motors are switched off the vehicle hits the surface with the others two landers and slides down along the surface.

In order to make the attitude parallel to the surface, one can try to move the desired landing point along the normal to the surface. Placing the desired landing point above the surface, the vehicle will fly in the desired position without even touching it. On the other hand, placing the desired landing position below the surface, we obtain a result opposite with respect to the desired one. In fact, trying to reach the desired position the vehicle tilts toward the surface (see Fig. 3b) instead of adjusting the attitude according to the plane. Moreover, at a certain moment of the experiment, the two landers in contact with the surface loose the grip and the vehicle crashes on it.

In general we also noticed a high flight instability when close to the surface due to aerodynamic effects.

### B. Sinusoidal trajectories

In order to validate and test the performances of the proposed hierarchical controller we tried to track some highly dynamical trajectories showing the ability to independently track $\varphi$ and $\vartheta_A$, at the same time.

In particular we shall show the results of the control action for three different sinusoidal trajectories: 1) sinusoidal trajectory with time varying frequency on $\varphi$ while keeping $\vartheta_A$ constant, 2) sinusoidal trajectory with time varying frequency on $\vartheta_A$ while keeping $\varphi$ constant, and 3) sinusoidal trajectory with fixed frequency on both $\varphi$ and $\vartheta_A$.

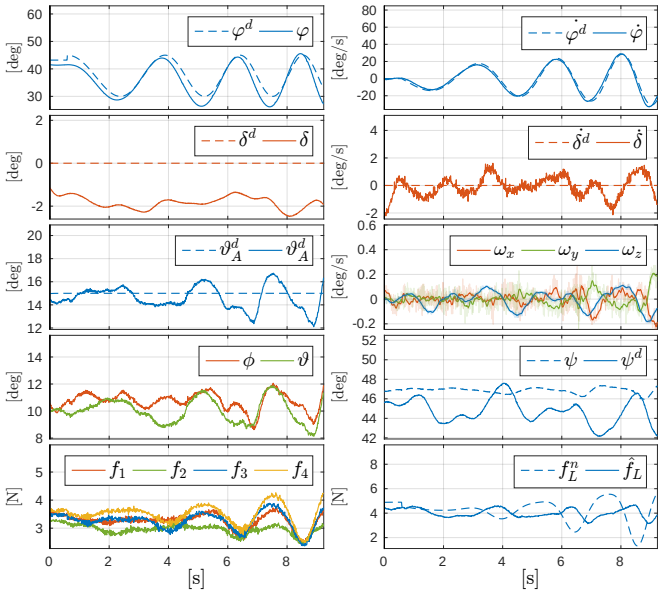



Fig. 4: Tracking of a sinusoidal input on elevation with varying period with fixed attitude

The first two tests are done firstly to see that the proposed controller can track a desired trajectory on $\varphi$ or $\vartheta_A$, independently. Secondly we want to show which is the maximum feasible frequency for both dynamics.

In the first experiment we fixed the desired $\vartheta_A^d$ at $15[^\circ]$. In this way we assured a sufficiently high tension in order to limit nominal negative tension value during the experiment. The desired sinusoidal trajectory $\varphi^d(t)$ starts with a frequency equal to $\omega_\varphi = \frac{2\pi}{4}\left[\frac{\text{rad}}{\text{s}}\right]$ and it increases linearly until the value of about $\omega_\varphi = \frac{4\pi}{5}\left[\frac{\text{rad}}{\text{s}}\right]$ for which the system becomes unstable. From Fig. 4 one can see that the tracking of $\varphi$ and $\vartheta_A$ degrades with the increasing of the frequency of the sinusoidal trajectory.

The second test is the dual, indeed we propose a sinusoidal desired trajectory with varying frequency on $\vartheta_A$ while keeping a desired constant $\varphi^d = 45[^\circ]$. For what concerns the frequency of the sinusoidal desired trajectory $\vartheta_A^d(t)$, it starts from a value of $\omega_{\vartheta_A} = \frac{2\pi}{6}\left[\frac{\text{rad}}{\text{s}}\right]$ and increase up to a value of about $\omega_{\vartheta_A} = \frac{8\pi}{9}\left[\frac{\text{rad}}{\text{s}}\right]$. After that, as it is possible to see from the plots in Fig. 5, the tracking error becomes very high. However, the system remains always stable.

Finally we gave as reference a sinusoidal trajectory on both $\varphi$ and $\vartheta_A$. The two signals have different frequency and phases, in particular $\omega_\varphi = \frac{2\pi}{4}\left[\frac{\text{rad}}{\text{s}}\right]$ and $\omega_{\vartheta_A} = \frac{2\pi}{6}\left[\frac{\text{rad}}{\text{s}}\right]$, respectively. The results can be seen in Fig. 6. As one can see the trajectories are both tracked with a sufficiently small error. This analysis finally shows that the proposed controller is able to independently track sufficiently slow time varying desired trajectories on both $\varphi$ and $\vartheta_A$, with small tracking errors. We did not report the results of the tracking of $\delta$ because they are analogous to the ones related to $\varphi$.

## REFERENCES


[1] M. Tognon, A. Testa, E. Rossi, and A. Franchi, "Takeoff and landing on slopes via inclined hovering with a tethered aerial robot," in *2016*

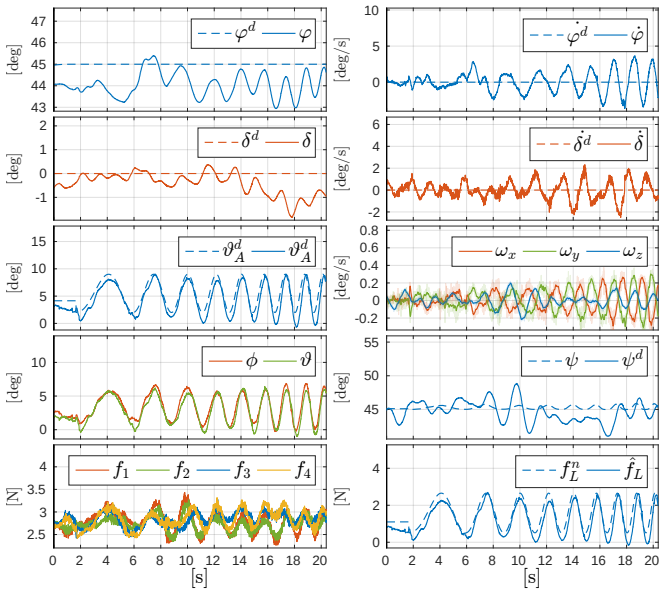



Fig. 5: Tracking of a desired sinusoidal trajectory of $\vartheta_A$ with varying frequency and fixed $\varphi$.

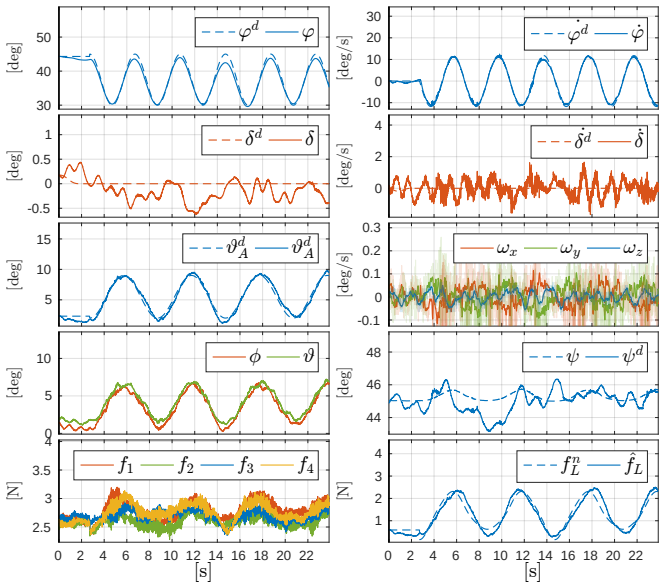



Fig. 6: Tracking of a desired sinusoidal trajectory on both $\varphi$ and $\vartheta_A$ with fixed period.


*IEEE/RSJ Int. Conf. on Intelligent Robots and Systems*, Daejeon, South Korea, Oct. 2016.

[2] M. Tognon and A. Franchi, "Nonlinear observer-based tracking control of link stress and elevation for a tethered aerial robot using inertial-only measurements," in *2015 IEEE Int. Conf. on Robotics and Automation*, Seattle, WA, May 2015, pp. 3994–3999.

[3] ——, "Dynamics, control, and estimation for aerial robots tethered by cables or bars," *CoRR*, vol. abs/1603.07567, 2016. [Online]. Available: http://arxiv.org/abs/1603.07567

[4] M. Tognon, S. S. Dash, and A. Franchi, "Observer-based control of position and tension for an aerial robot tethered to a moving platform," *IEEE Robotics and Automation Letters*, vol. 1, no. 2, pp. 732–737, 2016.

[5] M. Tognon and A. Franchi, "Control of motion and internal stresses for a chain of two underactuated aerial robots," in *14th European Control Conference*, Linz, Austria, Jul. 2015, pp. 1614–1619.

[6] ——, "Nonlinear observer for the control of bi-tethered multi aerial robots," in *2015 IEEE/RSJ Int. Conf. on Intelligent Robots and Systems*, Hamburg, Germany, Sep. 2015, pp. 1852–1857.

[7] B. Yüksel, C. Secchi, H. H. Bülthoff, and A. Franchi, "A nonlinear force observer for quadrotors and application to physical interactive tasks," in *2014 IEEE/ASME Int. Conf. on Advanced Intelligent Mechatronics*, Besançon, France, Jul. 2014, pp. 433–440.

[8] ——, "Reshaping the physical properties of a quadrotor through IDA-PBC and its application to aerial physical interaction," in *2014 IEEE Int. Conf. on Robotics and Automation*, Hong Kong, China, May. 2014, pp. 6258–6265.

[9] S. Rajappa, M. Ryll, H. H. Bülthoff, and A. Franchi, "Modeling, control and design optimization for a fully-actuated hexarotor aerial vehicle with tilted propellers," in *2015 IEEE Int. Conf. on Robotics and Automation*, Seattle, WA, May 2015, pp. 4006–4013.

[10] M. Ryll, D. Bicego, and A. Franchi, "Modeling and control of FAST-Hex: a fully-actuated by synchronized-tilting hexarotor," in *2016 IEEE/RSJ Int. Conf. on Intelligent Robots and Systems*, Daejeon, South Korea, Oct. 2016.

[11] M. Mohammadi, A. Franchi, D. Barcelli, and D. Prattichizzo, "Cooperative aerial tele-manipulation with haptic feedback," in *2016 IEEE/RSJ Int. Conf. on Intelligent Robots and Systems*, Daejeon, South Korea, Oct. 2016.

[12] G. Gioioso, A. Franchi, G. Salvietti, S. Scheggi, and D. Prattichizzo, "The Flying Hand: a formation of uavs for cooperative aerial tele-manipulation," in *2014 IEEE Int. Conf. on Robotics and Automation*, Hong Kong, China, May. 2014, pp. 4335–4341.

[13] G. Gioioso, M. Mohammadi, A. Franchi, and D. Prattichizzo, "A force-based bilateral teleoperation framework for aerial robots in contact with the environment," in *2015 IEEE Int. Conf. on Robotics and Automation*, Seattle, WA, May 2015, pp. 318–324.

[14] B. Yüksel, N. Staub, and A. Franchi, "Aerial robots with rigid/elastic-joint arms: Single-joint controllability study and preliminary experiments," in *2016 IEEE/RSJ Int. Conf. on Intelligent Robots and Systems*, Daejeon, South Korea, Oct. 2016.

[15] B. Yüksel, G. Buondonno, and A. Franchi, "Differential flatness and control of protocentric aerial manipulators with any number of arms and mixed rigid-/elastic-joints," in *2016 IEEE/RSJ Int. Conf. on Intelligent Robots and Systems*, Daejeon, South Korea, Oct. 2016.

[16] B. Yüksel, S. Mahboubi, C. Secchi, H. H. Bülthoff, and A. Franchi, "Design, identification and experimental testing of a light-weight flexible-joint arm for aerial physical interaction," in *2015 IEEE Int. Conf. on Robotics and Automation*, Seattle, WA, May 2015, pp. 870–876.

[17] A. Censi, A. Franchi, L. Marchionni, and G. Oriolo, "Simultaneous maximum-likelihood calibration of odometry and sensor parameters," *IEEE Trans. on Robotics*, vol. 29, no. 2, pp. 475–492, 2013.

[18] M. Tognon, A. Testa, E. Rossi, and A. Franchi, "Extended experiments for robust takeoff and landing on slopes exploiting a passive tether," LAAS-CNRS, Tech. Rep. hal-01349743, July 2016.